DOI: 10.31534/engmod.2022.2.ri.02m
Original scientific paper
Received: 07.06.2021.

Mathematical Modelling of Swallowing of Viscoelastic Nature Food Through the Oesophagus Affected by Hiatus Hernia

Vijay Kumar Shukla

Department of Mathematics, Shiv Harsh Kisan P.G. College, Basti - 272001, INDIA
e-mail: vshukla1100@gmail.com

SUMMARY

Peristaltic transport of viscoelastic fluid through a divergent tube is studied by approximations of long wavelength and low Reynolds number. This type of study explains the interesting phenomenon of swallowing food bolus through the oesophagus affected by hiatus hernia. The amplitude of peristaltic waves is increase exponentially, the food bolus to be a viscoelastic fluid and the affected oesophagus a diverging tube. The expressions for axial and radial velocities, pressure and reflux limit are obtained. Both cases have been considered when the whole tube diverges and when it diverges only near the end. Another case in which the tube converges near the last end has also been analysed.

KEY WORDS: *peristaltic transport; hiatus hernia; viscoelastic fluid; diverging tube; tube gradient.*

1. INTRODUCTION

The hiatus hernia is one of the most common diseases in the human body. In the case of hiatus hernia, the upper part of the stomach protrudes the chest through an opening of the diaphragm called the oesophageal hiatus. The lower part of the oesophagus then amplifies. Since the movement of food bolus through the oesophagus occurs due to peristaltic transport, during modelling of movement of food bolus through the oesophagus affected by hiatus hernia it is necessary to consider the gradual amplification in the radius of its lower part. Roman et al. [1] studied the diagnosis and management of hiatus hernia. Richter et al. [2] examine the variability of pressures with age and frequency of abnormal contractions.

Shapiro et al. [3] and Li and Brasseur [4] studied peristaltic transport in infinite and finite length tubes, respectively. Batra [5], Guha and Ahmad [6] investigated peristaltic transport through vas deferens with supposition that the ejaculatory phase occurs due to contraction and the nonejaculatory phase due to epididymal pressure and peristalsis. Jaffrin [7] discussed inertia and streamline curvature effects on peristaltic pumping. Gupta and Seshadri [8]

analyzed peristaltic pumping in non-uniform tubes. Hariharan et al. [9] studied the peristaltic transport of power law and Bingham fluid in a diverging tube with different wave forms as sinusoidal, multi-sinusoidal, triangular, trapezoidal and square waves and employed Fourier series to get the equations and results. Eytan et al. [10] developed a model of wall-induced fluid flow within a tapered two-dimensional channel and simulate intrauterine fluid flow. They showed that the transport phenomena are strongly dependent on the phase shift of wall displacement and the angle between the walls. They also discussed cases of reflux and trapping in a tapered channel. Misra and Pandey [11] investigated the peristaltic flow of a viscous incompressible Newtonian fluid through an axisymmetric circular tube of varying cross sections and used a perturbation technique to solve the problem. Further, Pandey and Chaube [12] discussed the peristaltic transport of viscoelastic fluid through an axisymmetric circular tube with varying cross sections. Pandey and Tripathi [13] also analyzed unsteady peristaltic transport of Maxwell fluid through a finite length tube.

Sankad et al. [14] studied the peristaltic transport of a Herschel-Bulkley fluid in a channel of the non-uniform cross section. They analysed the effects of these parameters on flow patterns for converging and diverging channels. Misra and Maiti [15] discussed the peristaltic motion of blood flow in the microcirculatory system in varying cross-section vessels. They assumed the blood as a Herschel-Bulkley fluid and consider the progressive peristaltic waves as sinusoidal in nature. Jyothi et al. [16] investigated the unsteady peristaltic flow of a Jeffrey fluid in a uniform and non-uniform tube. They solved governing equations numerically for both cases and discussed the effect of several parameters on flow characteristics. Akbar [17] analysed the different characteristics of peristaltic flow of a nano-fluid in a diverging tube and assumed the fluid as viscoelastic fluid.

Kahrilas et al. [18] experimentally found a high-pressure zone in the lower part of the oesophagus. Further, Xia et al. [19] measured oesophageal wall thickness in contracted as well as the dilated state. Pandey et al. [20] modified the previous model with consideration that the upper part of the oesophagus is thicker in the dilated state and the lower part of the oesophagus is thicker in the contracted state. They also considered that the amplitude of peristaltic waves increased exponentially during propagation through the oesophagus. Pandey and Tiwari [21] studied the swallowing of Casson fluid through the oesophagus under the influence of peristaltic waves of varying amplitude. Murad and Abdulhadi [22] discussed peristaltic transport of power-law fluid in an elastic tapered tube with variable cross-section induced by dilating peristaltic wave and showed that the flux is sinusoidal in nature.

Fluids such as bread and white eggs are considered viscoelastic fluids by Barnes et al. [23]. Sahin and Sumnu [24] assumed wheat flour dough, dairy cream, ice cream mix, marshmallow cream and cheese as viscoelastic fluid. Sweet potato puree is also observed as viscoelastic fluid by Ahmed and Ramaswamy [25]. Afoakwa et al. [26] supposed fermented maize as viscoelastic fluid. Further, above mentioned swallowing food is considered as viscoelastic Maxwell fluid.

Spurred by the above studies, a new model is constructed to study the swallowing food through the oesophagus affected by hiatus hernia disease with the consideration above results [18, 19, 20]. Oesophagus is assumed as an axisymmetric diverging tube, and the amplitude of peristaltic waves increases exponentially during propagation.

2. MATHEMATICAL FORMULATION

In this paper, peristaltic waves propagate with exponentially increasing amplitude along the walls of the diverging tube. The shape of the walls is changed as [20]:

$$h'(x',t') = a + b'x' - \phi' e^{k'x'} \cos^2 \frac{\pi}{\lambda}(x' - ct'), \tag{1}$$

where h' is the radial displacement of walls from the centre line, x' is the axial coordinate, t' is the time, a is the radius of the tube, ϕ' is the amplitude of the wave, k' the amplitude dilation parameter, λ is the wavelength, c is the wave velocity, and b' is a constant which depends on the length of the tube and dimensions of inlet and outlet radius of the tube.

The constitutive equation of Maxwell fluid is given as:

$$\left(1 + t'_m \frac{\partial}{\partial t\prime}\right)\tau' = \mu\dot{\gamma}', \tag{2}$$

where μ is the coefficient of viscosity, t'_m is the relaxation time, τ' is the extra stress tensor and $\dot{\gamma}'$ is the rate of strain.

The governing equations of the Maxwell fluid through the diverging tube are expressed as:

$$\frac{\partial u\prime}{\partial x\prime} + \frac{1}{r\prime}\frac{\partial(r\prime v\prime)}{\partial r\prime} = 0, \tag{3}$$

$$\rho\left(1 + t'_m \frac{\partial}{\partial t\prime}\right)\left(\frac{\partial u\prime}{\partial t\prime} + u'\frac{\partial u\prime}{\partial x\prime} + v'\frac{\partial u\prime}{\partial r\prime}\right) = -\left(1 + t'_m \frac{\partial}{\partial t\prime}\right)\frac{\partial p\prime}{\partial x'} + \mu\left(\frac{1}{r\prime}\frac{\partial}{\partial r\prime}\left(r'\frac{\partial u\prime}{\partial r\prime}\right) + \frac{\partial^2 u\prime}{\partial x\prime^2}\right), \tag{4}$$

$$\rho\left(1 + t'_m \frac{\partial}{\partial t\prime}\right)\left(\frac{\partial v\prime}{\partial t\prime} + u'\frac{\partial v\prime}{\partial x\prime} + v'\frac{\partial v\prime}{\partial r\prime}\right) = -\left(1 + t'_m \frac{\partial}{\partial t'}\right)\frac{\partial p'}{\partial r'} + \mu\left(\frac{\partial}{\partial r'}\left(\frac{1}{r'}\frac{\partial(r'v')}{\partial r'}\right) + \frac{\partial^2 v'}{\partial x'^2}\right), \tag{5}$$

where ρ is the fluid density, r' is the radial coordinate, u' is the axial velocity, v' is the radial velocity and p' represents the pressure.

The following parameters are introduced to transform the governing equations into a non-dimensional form:

$$\begin{cases} x = \frac{x\prime}{\lambda}, r = \frac{r'}{a}, t = \frac{ct\prime}{\lambda}, t_m = \frac{ct\prime_m}{\lambda}, u = \frac{u\prime}{c}, \\ v = \frac{v\prime}{c\alpha}, h = \frac{h\prime}{a}, l = \frac{l\prime}{\lambda}, \phi = \frac{\phi\prime}{a}, p = \frac{p\prime a^2}{\mu c\lambda}, \\ \alpha = \frac{a}{\lambda}, \psi = \frac{\psi\prime}{\pi a^2 c}, Q = \frac{Q\prime}{\pi a^2 c}, Re = \frac{\rho c a\alpha}{\mu}. \end{cases} \tag{6}$$

where α is the wave number, l' is the tube length, ψ' is the stream function, Q' is the volume flow rate, Re is the Reynolds number, and left side parameters are in non-dimensional form.

Using the parameters (6) in (1) to (5), the wave and governing equations are given as:

$$h(x,t) = 1 + bx - \phi e^{kx} \cos^2 \pi(x - t), \tag{7}$$

$$\frac{\partial u}{\partial x} + \frac{1}{r}\frac{\partial(rv)}{\partial r} = 0, \tag{8}$$

$$\left(1 + t_m \frac{\partial}{\partial t}\right)\left(\frac{\partial u}{\partial t} + u\frac{\partial u}{\partial x} + v\frac{\partial u}{\partial r}\right) = -\frac{1}{Re}\left(1 + t_m \frac{\partial}{\partial t}\right)\frac{\partial p}{\partial x} + \frac{1}{Re}\left(\frac{1}{r}\frac{\partial}{\partial r}\left(r\frac{\partial u}{\partial r}\right) + \alpha^2\frac{\partial^2 u}{\partial x^2}\right), \tag{9}$$

$$\left(1 + t_m \frac{\partial}{\partial t}\right)\left(\frac{\partial v}{\partial t} + u\frac{\partial v}{\partial x} + v\frac{\partial v}{\partial r}\right) = -\frac{1}{Re\alpha^2}\left(1 + t_m \frac{\partial}{\partial t}\right)\frac{\partial p}{\partial r} + \frac{1}{Re}\left(\frac{\partial}{\partial r}\left(\frac{1}{r}\frac{\partial(rv)}{\partial r}\right) + \alpha^2\frac{\partial^2 v}{\partial x^2}\right). \tag{10}$$

where $k(= k'\lambda)$ and $b\left(= \frac{\lambda b\prime}{a}\right)$ are constants.

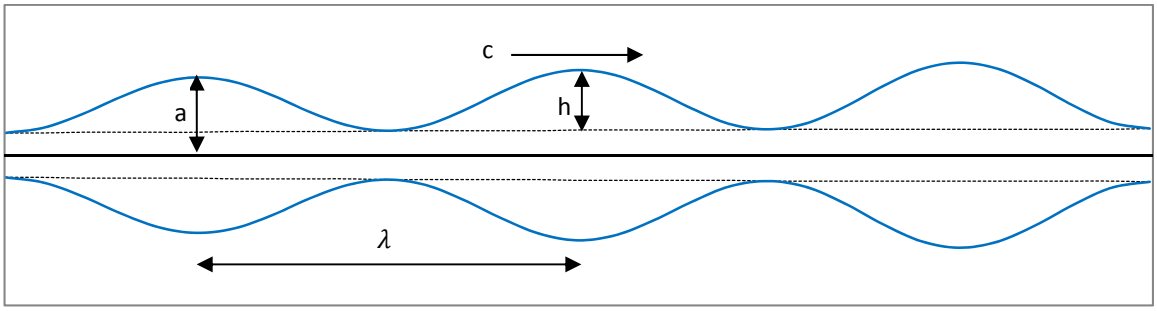

Fig. 1 *Phase portrait of propagation of the peristaltic waves along the wall of the oesophagus. a,h,c and λ represent the radius of the tube, the wall displacement due to wave propagation, the wave velocity, the wavelength of the wave respectively.*

Introducing the low Reynolds number and long wavelength approximations, the Eqs. from (8) to (10) can be written as:

$$\frac{\partial u}{\partial x}+\frac{1}{r}\frac{\partial (rv)}{\partial r}=0, \tag{11}$$

From Eq. (11) with boundary condition (16), the above equation becomes:

$$\frac{r^2}{2}\frac{\partial u}{\partial x}+rv=0, \tag{11'}$$

$$\left(1+t_m\frac{\partial}{\partial t}\right)\frac{\partial p}{\partial x}=\frac{\partial^2 u}{\partial r^2}+\frac{1}{r}\frac{\partial u}{\partial r} \tag{12}$$

$$\left(1+t_m\frac{\partial}{\partial t}\right)\frac{\partial p}{\partial r}=0. \tag{13}$$

Further, introducing the following boundary and regularity conditions:

$$u(x,r,t)|_{r=h}=0, \tag{14}$$

$$v(x,r,t)|_{r=h}=\frac{\partial h(x,t)}{\partial t}, \tag{15}$$

$$v(x,r,t)|_{r=0}=0, \tag{16}$$

$$\frac{\partial u(x,r,t)}{\partial r}|_{r=0}=0. \tag{17}$$

Pressures at the both ends of the tube are assumed as:

$$p|_{x=0}=p_0, p|_{x=l}=p_l. \tag{18}$$

Introducing the boundary conditions (14) and (17) in Eq. (12), the axial velocity is obtained as:

$$u=\frac{1}{4}[r^2-Z(x,t)]\left(1+t_m\frac{\partial}{\partial t}\right)\frac{\partial p}{\partial x} \tag{19}$$

where

$$Z(x,t)=\phi^2 e^{2\,k\,x}\cos^4\pi(x-t)-2\phi(1+bx)e^{k\,x}\cos^2\pi(x-t)+b^2x^2+2\,bx+1.$$

Further, the derivative of u w.r.t. to x, is expressed as:

$$\frac{\partial u}{\partial x}=\frac{1}{4}[r^2-Z(x,t)]\frac{\partial}{\partial x}\left\{\left(1+t_m\frac{\partial}{\partial t}\right)\frac{\partial p}{\partial x}\right\}-\frac{1}{4}\frac{\partial Z}{\partial x}\left(1+t_m\frac{\partial}{\partial t}\right)\frac{\partial p}{\partial x} \tag{19'}$$

where

$$\frac{\partial Z}{\partial x}=[1+bx-\phi e^{kx}\cos^2\pi(x-t)]\{2b-2\phi k e^{kx}\cos^2\pi(x-t)+2\phi\pi e^{kx}\sin 2\pi(x-t)\}.$$

From (11') with the use of the boundary condition (16) and substituting (19'), the radial velocity is obtained as:

$$v=\frac{r}{4}\left[\frac{1}{2}\frac{\partial Z}{\partial x}\left(1+t_m\frac{\partial}{\partial t}\right)\frac{\partial p}{\partial x}-\frac{1}{4}[r^2-2Z(x,t)]\frac{\partial}{\partial x}\left\{\left(1+t_m\frac{\partial}{\partial t}\right)\frac{\partial p}{\partial x}\right\}\right]. \tag{20}$$

Using boundary condition (15) in (20), the $\frac{\partial h}{\partial t}$ is expressed as:

$$\frac{\partial h(x,t)}{\partial t} = \frac{h(x,t)}{8}\left[\frac{\partial Z(x,t)}{\partial x}\left(1 + t_m \frac{\partial}{\partial t}\right)\frac{\partial p}{\partial x} + \frac{1}{2}Z(x,t)\frac{\partial}{\partial x}\left\{\left(1 + t_m \frac{\partial}{\partial t}\right)\frac{\partial p}{\partial x}\right\}\right]. \quad (21)$$

Now, integrate Eq. (21) the pressure gradient is expressed as follows:

$$\frac{\partial p}{\partial x} = e^{-\frac{t}{t_m}}\left[\frac{\partial p}{\partial x}|_{t=0} + \frac{1}{t_m}\int_0^t e^{\frac{t}{t_m}}\frac{\left\{\beta(t) + 8\int_0^x \frac{\partial Z(x,t)}{\partial t}dx\right\}}{Z^2(x,t)}dt\right], \quad (22)$$

where $\frac{\partial p}{\partial x}|_{t=0}$ is the pressure gradient at $t = 0$, and $\beta(t)$ is an arbitrary function of t. Integrating Eq. (22) from 0 to x, the pressure is:

$$p(x,t) - p(0,t) = e^{-\frac{t}{t_m}}\left[p(x,0) - p(0,0) + \frac{1}{t_m}\int_0^x \int_0^t e^{\frac{t}{t_m}}\frac{\left\{\beta(t) + 8\int_0^x \frac{\partial Z(x,t)}{\partial t}dx\right\}}{Z^2(x,t)}dtdx\right], \quad (23)$$

where $\beta(t)$ is expressed as:

$$\beta(t) = \frac{\left(1 + t_m\frac{\partial}{\partial t}\right)(p_l - p_0) - 8\int_0^l \frac{\int_0^x \frac{\partial Z(x,t)}{\partial t}dx}{Z^2(x,t)}dx}{\int_0^l \frac{1}{Z^2(x,t)}dx}. \quad (24)$$

2.1 VOLUME FLOW RATE

The volume flow rate is derived as $q(x,t) = \eta\int_0^h 2rudr$.

where $\eta = 1$ for the train waves and $\eta = \frac{l}{\lambda}$ for the single waves. In view of Eq. (19), $q(x,t)$is given by:

$$\begin{aligned} q(x,t) &= \eta\int_0^h 2r\left[\frac{1}{4}\{r^2 - Z(x,t)\}\left(1 + t_m\frac{\partial}{\partial t}\right)\frac{\partial p}{\partial x}\right]dr, \\ &= \frac{\eta}{4}\left\{\frac{h^4}{2} - h^2 Z(x,t)\right\}\left(1 + t_m\frac{\partial}{\partial t}\right)\frac{\partial p}{\partial x} \end{aligned} \quad (25)$$

To transform from laboratory frame to wave frame, the following transformations are further used:

$$\begin{cases} X = x - t, R = r, U = u - 1, V = v, \\ Q(X) = q(x,t) + Z(x,t). \end{cases} \quad (26)$$

The time average volume flow rate in wave frames is defined as:

$$\bar{Q}(X) = q(x,t) + \frac{3}{8}\phi^2 e^{2\,kx} - \phi(1 + bx)e^{kx} + b^2x^2 + 2bx + 1.$$

The average time volume flow rate in the laboratory frames is given as:

$$\bar{Q}(X) = Q(X) + \frac{3}{8}\phi^2 e^{2\,kx} - \phi(1 + bx)e^{kx} + b^2x^2 + 2bx + 1 - Z(x,t). \quad (27)$$

Now, in the term of volume flow rate, pressure is expressed as:

$$p(x,t) - p(0,t) = e^{-\frac{t}{t_m}}\left[p(x,0) - p(0,0) - \frac{8}{\eta\, t_m}\int_0^x \int_0^t e^{\frac{t}{t_m}}\frac{Q(x,t)}{Z^2(x,t)}dtdx\right]. \quad (28)$$

2.2 REFLUX LIMIT

The dimensional form of the stream function is given as:

$$d\psi' = 2\pi R'(U'dR' - V'dX') \quad (29)$$

Using the Eqs. (19), (20) and (26) in (29), the dimensionless stream function is obtained as:

$$\psi = \frac{\{2r^2Z(x,t)-Z^2(x,t)\}\left(\bar{Q}-\frac{3}{8}\phi^2 e^{2kx}+\phi(1+bx)e^{kx}-b^2x^2-2bx-1+Z(x,t)\right)}{Z^2(x,t)} - r^2. \quad (30)$$

The stream function at the wall is:

$$\psi|_{r=h} = \psi_w = \bar{Q} - \frac{3}{8}\phi^2 e^{2kx} + \phi(1+bx)e^{kx} - b^2x^2 - 2bx - 1. \quad (31)$$

The reflux volume flow rate is defined as:

$$Q_\psi = \psi + r^2(\psi, x) \quad (32)$$

The average reflux volume flow rate may be evaluated from (32) and obtained as:

$$\bar{Q}_\psi = \psi + \frac{1}{\eta}\int_0^\eta r^2(\psi, x)dx \quad (33)$$

The coefficients of the second and third terms in the expansion of $r^2(\psi, x) = h^2 + a_1\xi + a_2\xi^2 + \cdots$ are expressed as:

$$\begin{cases} a_1 = -1, \\ a_2 = -\frac{\bar{Q}-\frac{3}{8}\phi^2 e^{2kx}+\phi(1+bx)e^{kx}-b^2x^2-2bx-1+Z(x,t)}{Z^2(x,t)} \end{cases} \quad (34)$$

Finally, the reflux limit is expressed as:

$$\bar{Q} < \frac{3}{8}\phi^2 e^{2kx} - \phi(1+bx)e^{kx} + b^2x^2 + 2bx + 1 - \frac{\int_0^\eta \frac{1}{Z(x,t)}dx}{\int_0^\eta \frac{1}{Z^2(x,t)}dx} \quad (35)$$

Since Eq. (35) does not involve t_m, the relaxation time does not have any impact on reflux.

3. NUMERICAL RESULTS AND DISCUSSION

In this section, the effect of different parameters on swallowing food bolus in the oesophagus suffering from hiatus hernia is studied. It has assumed that the cross section area of the oesophagus varies from the upper end to the lower end. Two cases of the effect of hiatus hernia have been analysed. In the first case, it has also assumed that hiatus hernia affected the whole oesophagus. In this situation, hiatus hernia is formed in intensive form and the cross section area of the oesophagus varies from the upper end. In the second case, only the lower part of the oesophagus is affected by hiatus hernia. So mild hiatus hernia occurs and only some parts of the oesophagus are affected by this disease. Therefore, the cross section area of the lower part of the oesophagus varies and the remaining parts are not affected. For simulation purposes, the oesophagus is assumed as a tube with varying cross-section area and the radius of the tube is $a(x) = a + bx$, where b represents the tube gradient. This study was carried out to investigate the effects of relaxation time, tube gradient and the amplitude dilation parameter on the flow pattern of the Maxwell fluid. Graphs of pressure difference against axial distance are plotted with free pumping. Further, to analyse the numerical results, C programming is used. For the entire discussion, it is considered that only one bolus moves through the oesophagus which is more appropriate for the study of non-Newtonian fluid.

3.1 EFFECT OF RELAXATION TIME ON THE PRESSURE WHEN WHOLE TUBE DIVERGES

To study the influence of relaxation time on the movement of Maxwell fluid, pressure curves are plotted in Figure 2(a-f). To discuss the behaviour of the solution numerically, the values of different parameters are considered to be $\phi = 0.9$, $b = 0.001$, $k = 0.005$, $l = 2$, and

$t \in \{0, 1\}$. In this study, the relaxation time is varied in the range $t_m \in \{0.01, 0.09\}$. To analyse the results, it is assumed that the oesophagus carries only a single bolus at an instant.

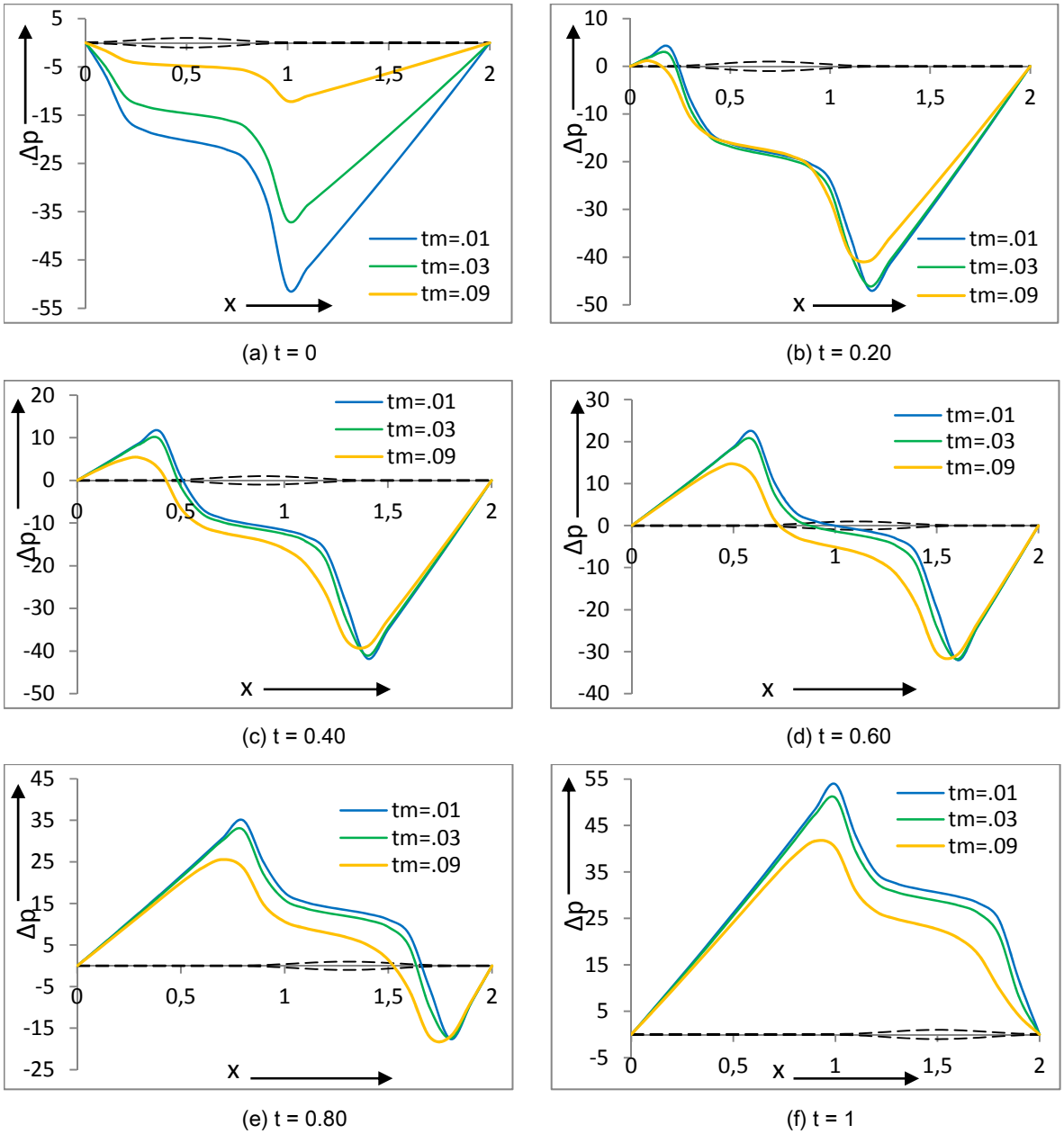

Fig. 2 *The diagrams display pressure vs. axial distance and dotted lines represent positions of bolus, and other lines show pressure distributions based on (23) corresponding to different relaxation times. The rest of the parameters are* $\phi = 0.9, b = 0.001, k = 0.005$ *and* $l = 2$.

3.2 EFFECT OF TUBE GRADIENT ON THE PRESSURE WHEN WHOLE TUBE DIVERGES

Pressure curves are plotted in Figure 3(a-f) to study the influence of tube gradient on swallowing food bolus through the oesophagus. The values of parameters are taken to be

$\phi = 0.9, k = 0.005, t_m = 0.03, l = 2$ and $b \in \{0, 0.01\}$ for the numerical study. It revealed that the pressure decreases with the increase of tube gradient.

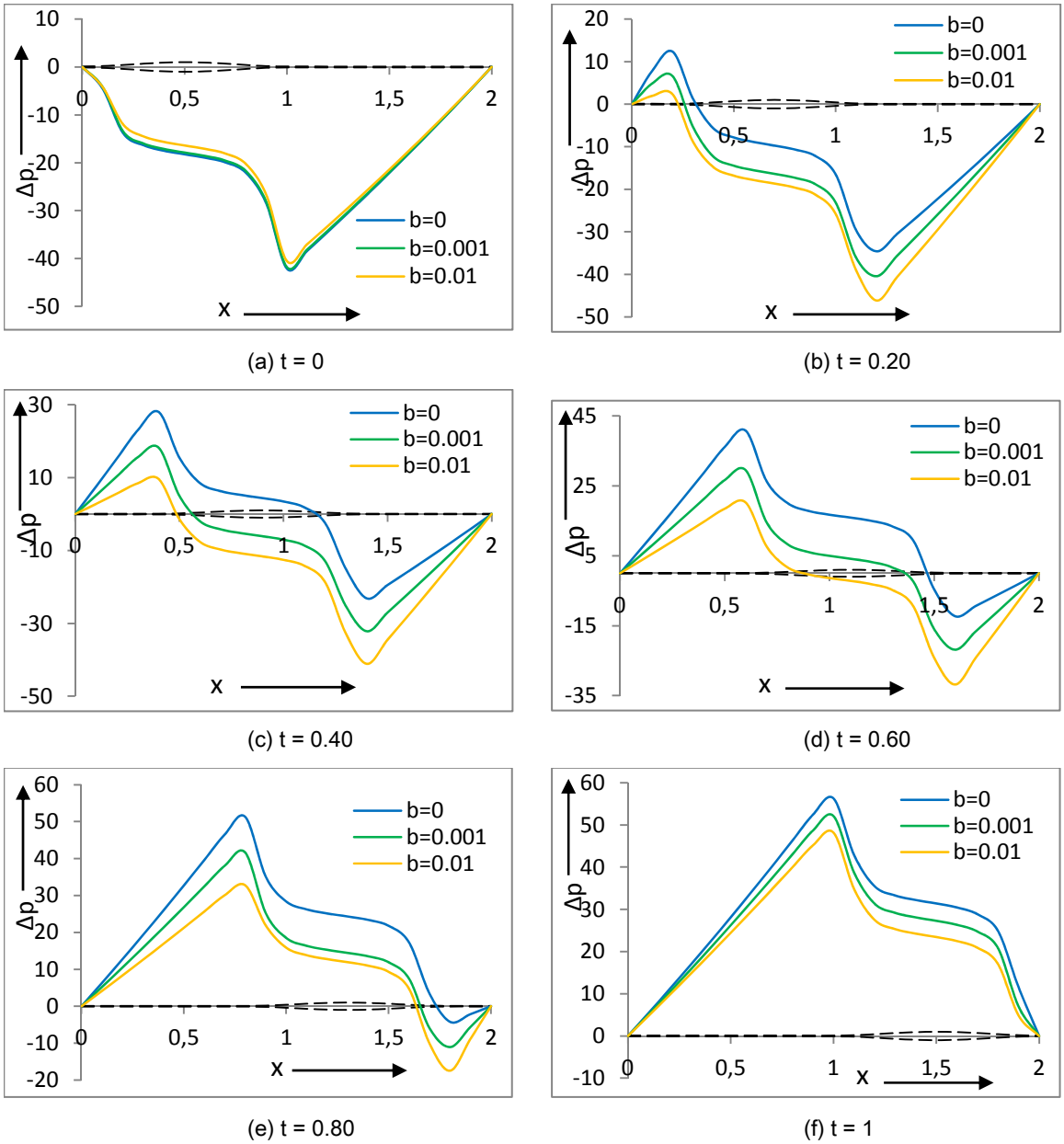

Fig. 3 *The diagrams display pressure vs. axial distance and dotted lines represent positions of bolus, and other lines show pressure distributions based on (23) corresponding to different tube gradients. The rest of the parameters are* $\phi = 0.9, k = 0.005, t_m = 0.03$ *and* $l = 2$.

3.3 EFFECT OF TUBE GRADIENT ON THE PRESSURE WHEN TUBE DIVERGES NEAR THE END

In this section, the lower part of the oesophagus affected by hiatus hernia disease and a single bolus moving through the tube with cross sectional diverges towards the end caused by the presence of mild hiatus hernia is observed (see Figure 4(a-d)). For the analysis, it is assumed

that the last part of the oesophagus diverges and pressure is measured at different $t \in \{0.11, 0.38, 0.67, 0.79\}$ and at $b \in \{0, 0.01, 0.1\}$. For $b = 0$, the tube is a uniform tube but at $b = 0.01$ & 0.1 , the tube diverges. The wave amplitude dilation factor is fixed at $k = 0.005$.

For $t = 0.11$ (see Figure 4(a)), observation of the pressure curves depict that the pressure in a diverging tube (i.e., $b = 0.01$ & 0.1) rises more than that in the uniform tube (i.e.$b = 0$), but falls less than that in the uniform tube, although the divergence is located towards the end. Further, the pressure required for flow in the diverging tube is lower than that in the uniform tube. It is also found that the pressure rises to zero in all the cases but in the uniform tube, the pressure rises linearly while it rises concavely when the tube diverges towards the end. For $t = 0.38$ (see Figure 4(b)), when the bolus is farther from the initial end, pressure curves depict similar behaviour with $t = 0.11$. At this instant, the magnitude of the pressure difference is much smaller than in the previous case. At $t = 0.67$(see Figure 4(c)), bolus passes the middle of the tube and pressure in a diverging tube (i.e., $b = 0.01$ & 0.1) rises less than that in the uniform tube (i.e. $b = 0$) but falls more than that in the uniform tube. It is also observed that the magnitude of the pressure is greater in the case of the uniform tube and lower in diverges tube. At $t = 0.79$, the bolus is near the outlet and is situated where the tube actually diverges. Pressure rises here but it is lower in comparison for the divergent than the uniform tube. Although the tube diverges toward the end only, its impact is felt on the pressure distribution starting from the beginning.

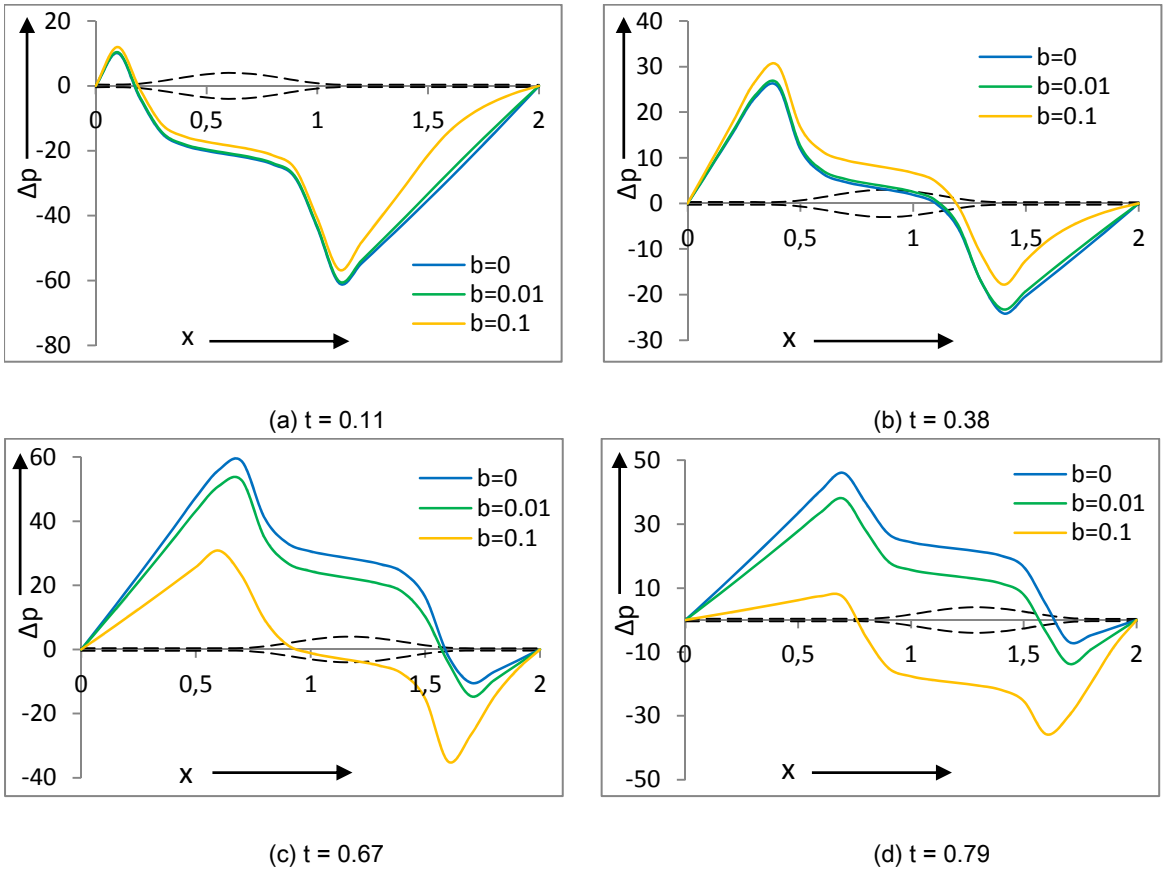

Fig. 4 *The diagrams display pressure vs. axial distance and dotted lines represent positions of bolus, and other lines show pressure distributions based on (23) corresponding to different tube gradients. The other parameters are* $\phi = 0.9, k = 0.005, t_m = 0.03$ *and* $l = 2$.

3.4 EFFECT OF TUBE GRADIENT ON THE PRESSURE WHEN TUBE CONVERGES NEAR THE END

Since in the case of hiatus hernia the stomach moves upward through the hiatus, for better modelling, it is more appropriate if the oesophagus is taken as a converging tube. For the analysis, the pressure difference is measured at $= \{0.11, 0.38, 0.67, 0.79\}$ and at the tube gradient $b = \{0, 0.01, 0.1\}$ for a fixed value of wave amplitude dilation factor $k = 0.005$ with the assumption that the end part of the oesophagus diverges. Although the convergence is located near the lower end, at $t = 0.11$ (see Figure 5(a)), it is observed that the pressure in a converging tube (i.e., $b = 0.01$ & 0.1) rises less than that in the uniform tube (i.e.$b = 0$), but falls more. It is also visualized from the figure that more pressure is required for the flow in the converging tube than for the uniform tube. It is also shown that the pressure rises to zero in all the cases but in the converging tube, pressure rise convexly while in the uniform tube it rises linearly. At $t = 0.38$ (see Figure 5(b)), the food bolus moves farther from the initial end. At this instant, the magnitude of the pressure difference is much smaller than in the previous case. Bolus passes the middle of the tube at $t = 0.67$(see Figure 5(c)), in this case pressure curves show that the pressure in a converging tube (i.e., $b = 0.01$ & 0.1) rises less than that in the uniform tube (i.e.$b = 0$), but falls more.

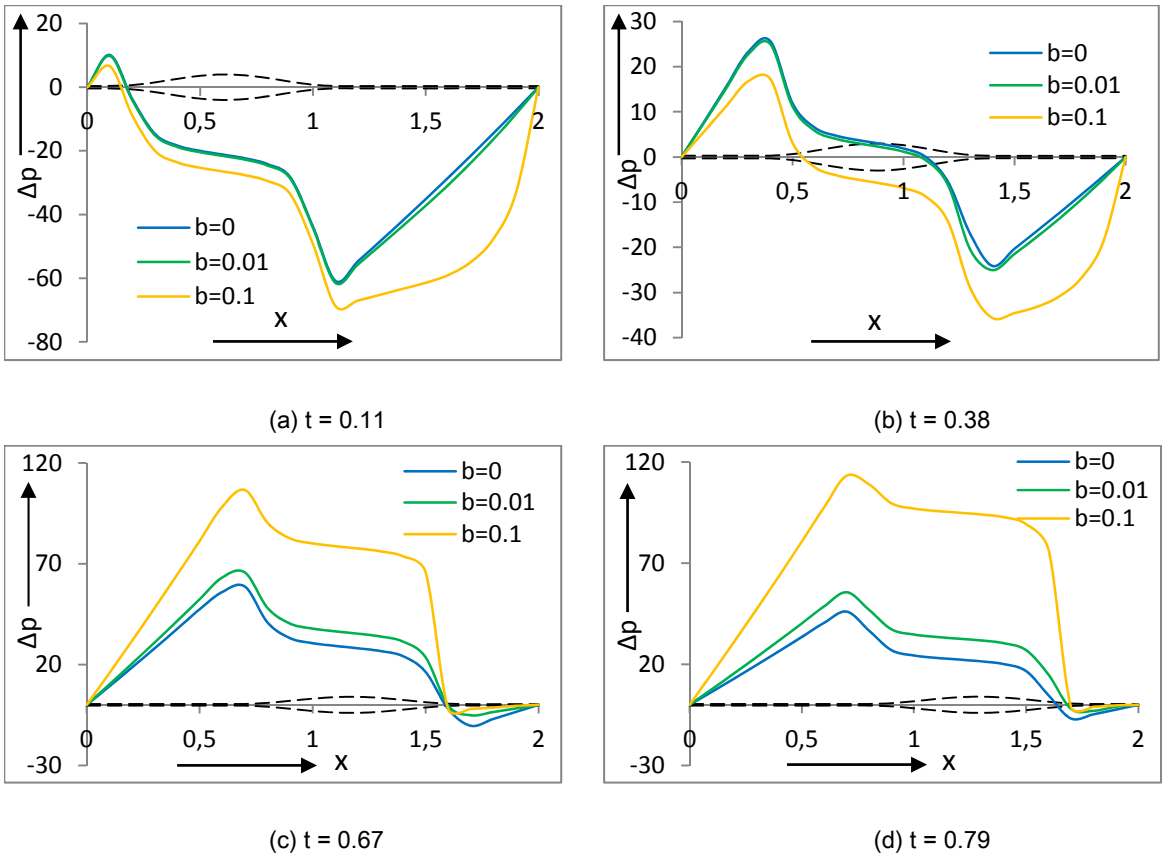

Fig. 5 *The diagrams display pressure vs. axial distance and dotted lines represent positions of bolus, and other lines show pressure distributions based on (23) corresponding to different tube gradients. The rest of the parameters are* $\phi = 0.9, k = 0.005, t_m = 0.03$ *and* $l = 2$.

It is also noted that the magnitude of the pressure difference is lower in the case of the uniform tube and greater in converges tube. At $t = 0.79$ the bolus reaches near the outlet and more pressure is required to push the bolus through this region, and with convergences, tube pressure difference also increases.

3.5 EFFECT OF AMPLITUDE DILATION ON THE PRESSURE WHEN WHOLE TUBE DIVERGES

The pressure difference is plotted in Figure 6 (a-f) to study the influence of amplitude dilation on swallowing food bolus through the oesophagus. For analysing the effect of amplitude dilation, the values of other parameters are taken as $\phi = 0.9, b = 0.001, t_m = 0.03, l = 2$ and $t \in \{0,1\}$. The amplitude dilation parameter is varied in the range $k \in \{0, 0.01\}$. It indicates that the pressure increases when the food bolus moves in the lower part of the oesophagus.

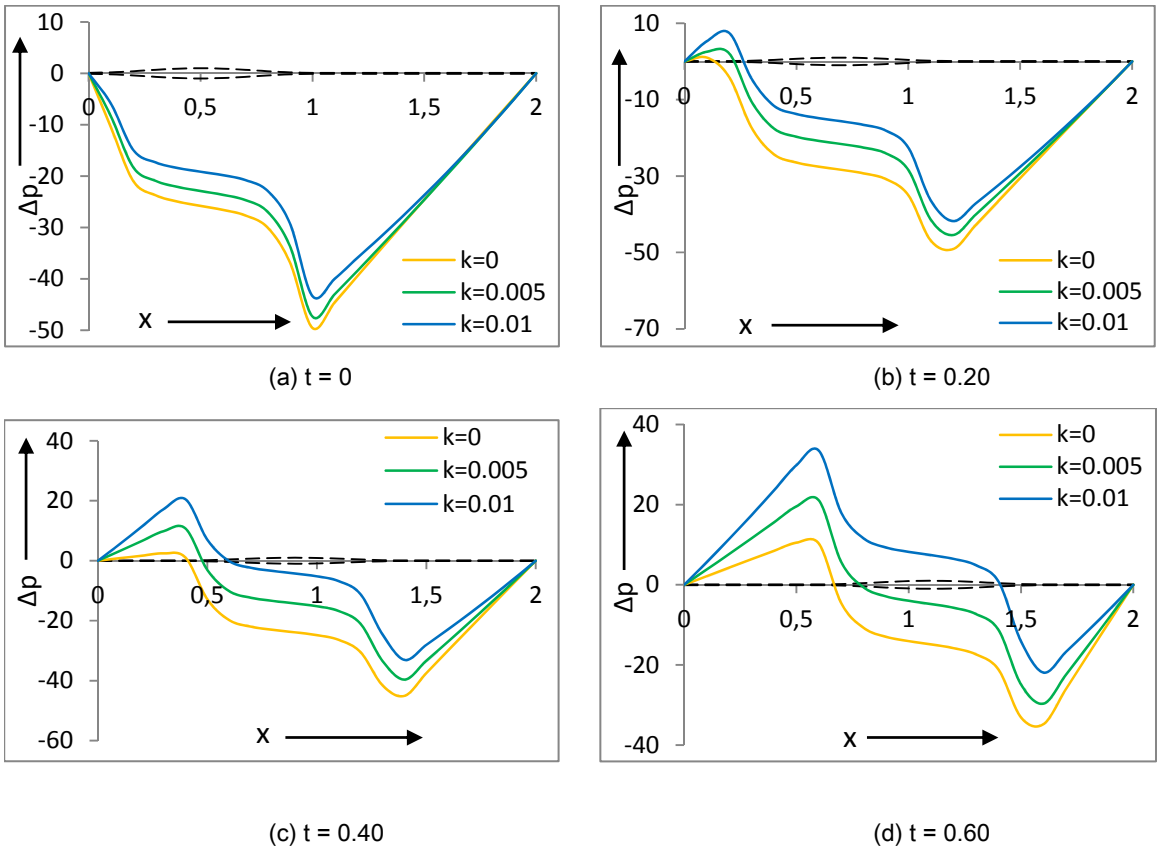

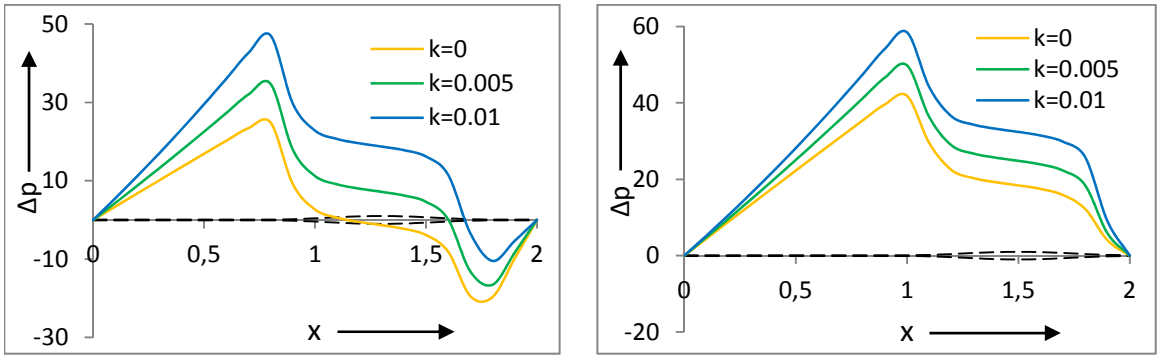

(e) t = 0.80 (f) t = 1

Fig. 6 *The diagrams display pressure vs. axial distance and dotted lines represent positions of bolus, and other lines show pressure distributions based on (23) corresponding to different amplitude dilation parameters. The rest of the parameters are* $\phi = 0.9, b = 0.001, t_m = 0.03$ *and* $l = 2$.

3.6 EFFECT OF TUBE GRADIENT ON REFLUX

The variations of average volume flow rate against amplitude ratio for different parameters are displayed in Figure 7. It is observed that the flow rate diminishes as the tube gradient b increases. These results are analysed for the values of $\phi = 0.9, k = 0.005, l = 2$ and $d \in \{0, 0.05\}$.

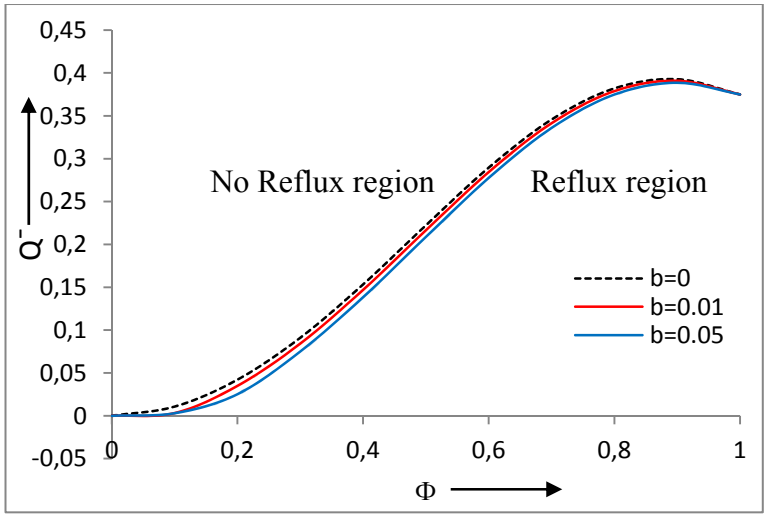

Fig. 7 *The diagram displays the average volume flow rate against the wave amplitude based on (35) corresponding to different tube gradients. The rest of the parameters are* $\phi = 0.9, k = 0.005, \eta = 0.5$ *and* $l = 2$.

3.7 EFFECT OF AMPLITUDE DILATION ON REFLUX

Plots between the amplitude ratio and the average volume flow rate for different values of tube gradient and amplitude dilation parameter are displayed in Figure 8. The investigation revealed that the flow rate increases as the amplitude dilation parameter increases. For this study, the value of parameters are $\phi = 0.9, b = 0.001, l = 2$ and the amplitude dilation parameter $k \in \{0, 0.09\}$.

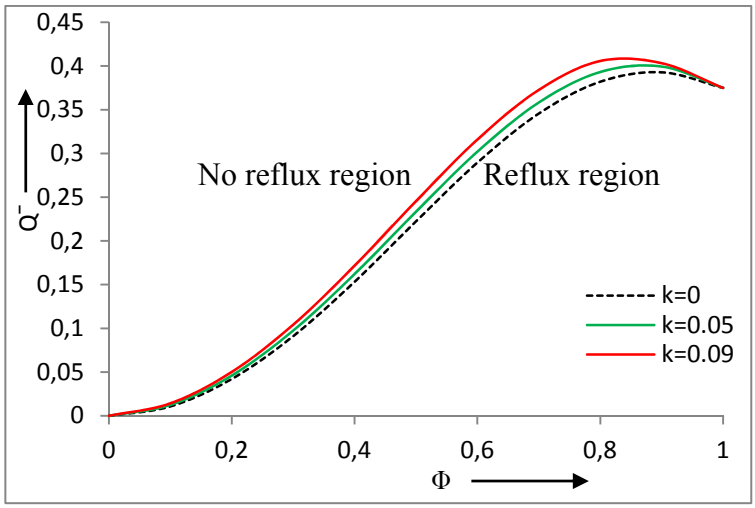

Fig. 8 *The diagram displays the average volume flow rate against the wave amplitude based on (35) corresponding to different amplitude dilation parameters. The rest of the parameters are* $\phi = 0.9, b = 0.001, \eta = 0.5$ *and* $l = 2$.

4. CONCLUSION

Peristaltic transport of viscoelastic fluid is analysed in circular cylinder diverging and converging tubes with the supposition that the length of the tube is finite. Both cases when the whole tube diverges and only near the end are discussed. For better modelling, another case in which the tube converges near the last end is also investigated.

It is observed that as the relaxation time increases, pressure decreases for the fixed value of other parameters if the whole tube diverges. But when the tube diverges near the last end, pressure varies concavely near the last end and when the tube converges near the last end, the pressure varies convexly. Moreover, when the tube gradient increases, pressure decreases but with the increase of the amplitude dilation parameter, the pressure difference increases.

In addition, it is concluded that the reflux region increases with the amplitude dilation parameter. The reflux region is also investigated for different tube gradients. It is also observed that the reflux region diminishes as tube gradient increases and relaxation time does not affect the reflux region. If the whole tube diverges, the relaxation time increases and pressure decreases. In contrast, when the tube diverges near the last end the pressure varies concavely near the last end.

Further, it is also investigated that when the tube gradient increases, pressure decreases, and when the amplitude dilation parameter increases, pressure difference increases too. Simultaneously, the reflux region increases with the amplitude dilation parameter and the reflux region diminishes with the increase of the tube gradient. The reflux region also increases with the amplitude dilation parameter but decreases when the tube diverges. It is also revealed that the relaxation time does not influence the reflux region even when the tube diverges.

5. ACKNOWLEDGMENT

Author thanks the anonymous reviewers and editors for their useful suggestions.

6. REFERENCES

[1] S. Roman, P.J. Kahrilas, The diagnosis and management of hiatus hernia, *BMJ,* Vol. 17, pp. 349, 2014. https://doi.org/10.1136/bmj.g6154

[2] J.E. Richter, W.C. Wu, D.N. Johns, J.N. Blackwell, J.L. Nelson III, J.A. Castell, D.O. Castell, Esophageal manometry in 95 healthy adult volunteers, *Digestive Diseases and Sciences*, Vol. 32, No. 6, pp. 583-592, 1987. https://doi.org/10.1007/BF01296157

[3] A.H. Shapiro, M.Y. Jaffrin, S.L. Weinberg, Peristaltic pumping with long wavelengths at low Reynolds number, *Journal of Fluid Mechanics*, Vol. 37, No. 4, pp. 799-825, 1969.

https://doi.org/10.1017/S0022112069000899

[4] M. Li, J.G. Brasseur, Non-steady peristaltic transport in finite-length tubes*, Journal of Fluid Mechanics*, Vol. 248, pp. 129-151, 1993.

https://doi.org/10.1017/S0022112093000710

[5] S.K. Batra, Sperm transport through vas deferens: review of hypotheses and suggestions for a quantitative model, *Fertility and Sterility*, Vol. 25, No. 2, pp. 186-202, 1974.

https://doi.org/10.1016/S0015-0282(16)40220-7

[6] S.K. Guha, H. Kaur, H. Ahmed, Mechanics of spermatic fluid transport in the vas deferens, *Medical and Biological Engineering,* Vol. 13, pp. 518–522, 1975.

https://doi.org/10.1007/BF02477128

[7] M.Y. Jaffrin, Inertia and streamline curvature effects on peristaltic pumping, *International Journal of Engineering Science*, Vol. 11, No. 6, pp. 681-699, 1973.

https://doi.org/10.1016/0020-7225(73)90029-3

[8] B.B. Gupta, V. Seshadri, Peristaltic pumping in non-uniform tubes, *Journal of Biomechanics*, Vol. 9, No. 2, pp. 105-109, 1976.

https://doi.org/10.1016/0021-9290(76)90130-5

[9] P. Hariharan, V. Seshadri, R.K. Banerjee, Peristaltic transport of non-Newtonian fluid in a diverging tube with different wave forms, *Mathematical and Computer Modelling*, Vol. 48, No. 7, pp. 998-1017, 2008. https://doi.org/10.1016/j.mcm.2007.10.018

[10] Eytan, A.J. Jaffa, D. Elad, Peristaltic flow in a tapered channel: application to embryo transport within the uterine cavity, *Medical Engineering & Physics*, Vol. 23, No. 7, pp. 475-484, 2001. https://doi.org/10.1016/S1350-4533(01)00078-9

[11] J.C. Misra, S.K. Pandey, A mathematical model for oesophageal swallowing of a food-bolus, *Mathematical and Computer Modelling*, Vol. 33, No. 8, pp. 997-1009, 2001.

https://doi.org/10.1016/S0895-7177(00)00295-8

[12] S.K. Pandey, M.K. Chaube, Peristaltic transport of a visco-elastic fluid in a tube of non-uniform cross section, *Mathematical and Computer Modelling*, Vol. 52, No. 3, pp. 501-514, 2010. https://doi.org/10.1016/j.mcm.2010.03.047

[13] S.K. Pandey, D. Tripathi, Unsteady peristaltic transport of Maxwell fluid through finite length tube: application to oesophageal swallowing, *Applied Mathematics and Mechanics*, Vol. 33, No. 1, pp. 15-24, 2012. https://doi.org/10.1007/s10483-012-1530-9

[14] G.C. Sankad, P.S. Nagathan, A. Patil, M.Y. Dhange, Peristaltic transport of a Herschel-Bulkley fluid in a non-uniform channel with wall effects, *International Journal of Engineering Science and Innovative Technology*, Vol. 3, No. 3, pp. 669-678, 2014.

[15] J.C. Misra, S. Maiti, Peristaltic pumping of blood through small vessels of varying cross-section, *Journal of Applied Mechanics*, Vol. 79, No. 6, pp. 61003-61021, 2012.

https://doi.org/10.1115/1.4006635

[16] N.N. Jyothi, P. Devaki, S. Sreenadh, High frequency unsteady peristaltic flow of a Jeffrey fluid in uniform and tapered tube, *Elixir Fluid Dynamics*, Vol. 60, pp. 16152-16166, 2013.

[17] N.S. Akbar, Peristaltic flow of a nanofluid in a diverging tube for Jeffrey fluid, *Journal of Computational and Theoretical nanoscience*, Vol. 11, No. 5, pp. 1335-1341, 2014.

https://doi.org/10.1166/jctn.2014.3501

[18] P.J. Kahrilas, S. Wu, S. Lin, P. Pouderoux, Attenuation of esophageal shortening during peristalsis with hiatus hernia, *Gastroenterology*, Vol. 109*,* No. 6, pp. 1818-1825. 1995. https://doi.org/10.1016/0016-5085(95)90748-3

[19] F. Xia, J. Mao, J. Ding, H. Yang, Observation of normal appearance and wall thickness of esophagus on CT images, *European Journal of Radiology*, Vol. 72, No. 3, pp. 406-411, 2009. https://doi.org/10.1016/j.ejrad.2008.09.002

[20] S.K. Pandey, G. Ranjan, S.K. Tiwari, K. Pandey, Variation of pressure from cervical to distal end of oesophagus during swallowing: Study of a mathematical model, *Mathematical Biosciences*, Vol. 288, pp. 149-158, 2017.

https://doi.org/10.1016/j.mbs.2017.03.010

[21] S.K. Pandey, S.K. Tiwari, Swallowing of Casson fluid in oesophagus under the influence of peristaltic waves of varying amplitude, *International Journal of Biomathematics*, Vol. 10, No. 2, 1750017, 2017. https://doi.org/10.1142/S1793524517500176

[22] M.A. Murad, A.M. Abdulhadi, Peristaltic transport of power-law fluid in an elastic tapered tube with variable cross-section induced by dilating peristaltic wave, *Iraqi Journal of Science*, Vol. 62, No. 4, pp. 1293-1306, 2021.

https://doi.org/10.24996/ijs.2021.62.4.25

[23] H.A. Barnes, J.F. Hutton, K. Walters, *An Introduction to Rheology,* Elsevier, 1st Edition, Vol. 3, 1989.

[24] S. Sahin, S.G. Sumnu, Rheological properties of food, *Physical Properties of Foods,* Springer Science & Business Media*,* 39-105, 2006.

[25] J. Ahmed, H.S. Ramaswamy, Viscoelastic properties of sweet potato puree infant food, *Journal of Food Engineering*, Vol. 74, No. 3, pp. 376-382, 2006.

https://doi.org/10.1016/j.jfoodeng.2005.03.010

[26] E.O. Afoakwa, R. Adjonu, J. Asomaning, Viscoelastic properties and pasting characteristics of fermented maize: influence of the addition of malted cereals, *International Journal of Food Science & Technology*, Vol. 45, No. 2, pp. 380-386, 2010.

https://doi.org/10.1111/j.1365-2621.2009.02160.x